

RESEARCH ARTICLE

New Insights on Non-Enzymatic Oxidation of Ganglioside GM1 Using Mass Spectrometry

Daniela Couto,¹ Tânia Melo,¹ Elisabete Maciel,^{1,2} Ana Campos,¹ Eliana Alves,¹ Sofia Guedes,¹ M. Rosário M. Domingues,¹ Pedro Domingues¹

¹Mass Spectrometry Center, Department of Chemistry and QOPNA, University of Aveiro, 3810-193, Aveiro, Portugal

²Department of Biology and CESAM, University of Aveiro, Campus Universitario de Santiago, 3810-193, Aveiro, Portugal



Abstract. Gangliosides are acidic glycosphingolipids that are present in cell membranes and lipid raft domains, being particularly abundant in central nervous systems. They participate in modulating cell membrane properties, cell–cell recognition, cell regulation, and signaling. Disturbance in ganglioside metabolism has been correlated with the development of diseases, such as neurodegenerative diseases, and in inflammation. Both conditions are associated with an increased production of reactive oxygen species (ROS) that can induce changes in the structure of biomolecules, including lipids, leading to the loss or modification of their function. Oxidized phospholipids are usually involved in chronic diseases and inflammation. However, knowledge regarding oxidation of gangliosides is scarce. In order to evaluate the

effect of ROS in gangliosides, an in vitro biomimetic model system was used to study the susceptibility of GM1 (Neu5Acα2-3(Galβ1-3GalNAcβ1-4)Galβ1-4Glcβ1Cer) to undergo oxidative modifications. Oxidation of GM1 under Fenton reaction conditions was monitored using high resolution electrospray ionization-mass spectrometry (ESI-MS) and tandem mass spectrometry (ESI-MS/MS). Upon oxidation, GM1 underwent oxidative cleavages in the carbohydrate chain, leading to the formation of other gangliosides GM2 (GalNAcβ1-4Gal(Neu5Acα2-3)1-4Glcβ1Cer), GM3 (Neu5Acα2-3Galβ1-4Glcβ1Cer), asialo-GM1 (Galβ1-3GalNAcβ1-4Galβ1-4Glcβ1Cer), asialo-GM2 (GalNAcβ1-4Galβ1-4Glcβ1Cer), of the small glycolipids lactosylceramide (LacCer), glucosylceramide (GlcCer), and of ceramide (Cer). In addition, oxygenated GM1 and GM2 (as keto and hydroxy derivatives), glycans, oxidized glycans, and oxidized ceramides were also identified. Nonenzymatic oxidation of GM1 under oxidative stress contributes to the generation of other gangliosides that may participate in the imbalance of gangliosides metabolism in vivo, through uncontrolled enzymatic pathways and, consequently, play some role in neurodegenerative processes.

Keywords: GM1, Reactive oxygen species, Fenton reaction, Neurodegenerative diseases, Inflammation, Electrospray ionization

Received: 1 March 2016/Revised: 27 July 2016/Accepted: 28 July 2016/Published Online: 30 August 2016

Introduction

Gangliosides or acidic glycosphingolipids (GSLs) belong to a heterogeneous class of lipids, that share a common hydrophobic ceramide (Cer) moiety linked to a hydrophilic oligosaccharide chain composed by, at least, one sialic acid residue. In human gangliosides, the most common sialic acid is

N-acetylneuraminic acid (NeuAc) [1]. Gangliosides are present in the outer leaflet of the cell membranes and are preferentially located in specialized microdomains, such as lipid rafts [2]. GSLs are vital for the maintenance of membrane organization and structure and also play important functions as cell–cell recognition, cell regulation, cell signaling, and intracellular protein trafficking (as reviewed in [3]). Still, it is known that the glycosphingolipid structure defines its immunostimulatory or immunosuppressive activity. For instance, the simpler gangliosides, with the simplest carbohydrate structures, such as GM2, GM3, and GM4, or α -galactosylceramide (not present in normal mammalian cells) are known as very active immunosuppressors [4–6].

Electronic supplementary material The online version of this article (doi:10.1007/s13361-016-1474-1) contains supplementary material, which is available to authorized users.

Correspondence to: Pedro Domingues; e-mail: p.domingues@ua.pt

The biosynthesis of gangliosides is rigorously controlled by enzymes, which maintain their profile narrowly regulated [7]. The profile of ganglioside depends on species, tissue, and cell-type tissues, and also changes depending on the cell cycle [8]. Gangliosides are more abundant in central nervous system (CNS), accounting for 10%–12% of its total lipid content [9]. Therefore, it is believed that gangliosides play crucial functions in the behavior, development, and maturation of the CNS [10, 11]. An abnormal expression, degradation, or distribution of these biomolecules has been associated with the development of pathologic conditions, such as inflammation, cancer, and neurodegenerative diseases [12]. In some neurodegenerative diseases such as amyotrophic lateral sclerosis (ALS), Niemann-Pick type C, Alzheimer's disease (AD), Parkinson's disease (PD), and gangliosidosis (intralysosomal accumulation of a ganglioside), it was observed that the gangliosides profile suffers alterations [13–15]. In AD, a decrease in some gangliosides was observed, while other gangliosides increased in multiple regions of the CNS, compared with age-matched control tissues [16]. So, these alterations may contribute to neurodegeneration and inflammation states observed in these disorders, due to the key functions of gangliosides in CNS.

Neurodegeneration is also associated with oxidative stress and, consequently, with an increased production of reactive oxygen species (ROS) [17]. It is well known that ROS cause changes in the structure of biomolecules, particularly to lipids, leading to the loss of their function and to development of diseases. Although the oxidation mediated by ROS has been extensively studied for polyunsaturated fatty acids (PUFAs), phospholipids [18–21], and sphingolipids [22–24], there are no reports on the oxidation of gangliosides. Gangliosides are quite abundant in CNS, which is particularly sensitive to oxidative stress, especially compared with other organs, because it has fewer antioxidant defense mechanisms [25]. In previous studies, the oxidation of sphingomyelin induced by hydroxyl radical led to lysosphingolipids and ceramides [22]. OH[•] radical-induced oxidation of galactosylceramide (GalCer) and lactosylceramide (LacCer) led to formation of oxygenated GalCer and LacCer species, ceramides, and oxidized ceramides [24]. Ceramides are considered to be important bioactive lipids because of their role in various biological processes, such as regulation of cell proliferation and apoptosis, among others [23, 26, 27].

The main goal of our work was to study the *in vitro* oxidation of the monoganglioside, Neu5Ac α 2-3(Gal β 1-3GalNAc β 1-4)Gal β 1-4Glc β 1Cer (GM1), induced by hydroxyl radicals generated under Fenton reaction. The oxidation was monitored by electrospray ionization-mass spectrometry (ESI-MS), tandem MS (MS/MS), and liquid chromatography (LC) coupled to ESI-MS. High resolution Q-Exactive Orbitrap was used to confirm the proposed structural assignments by exact mass measurements. The identification of the oxidation products of GM1 was based on the interpretation of high resolution MS and MS/MS data, obtained in the Orbitrap mass spectrometer. Exact mass accuracy measurements were used to confirm the proposed assignments.

Materials and Methods

Chemicals

GM1 standard was obtained from Avanti Polar Lipids, Inc. (Alabaster, AL, USA) and used without further purification. GM1 standard was a mixture of Neu5Ac α 2-3(Gal β 1-3GalNAc β 1-4)Gal β 1-4Glc β 1Cer (GM1, ceramide d18:1/C18:0), and Neu5Ac α 2-3(Gal β 1-3GalNAc β 1-4)Gal β 1-4Glc β 1Cer (GM1, ceramide d20:1/C18:0). HPLC grade chloroform (CHCl₃), methanol (MeOH) and acetonitrile were purchased from Fisher Scientific Ltd. (Leicestershire, UK). Ammonium hydrogenocarbonate, ethylenediaminetetraacetic acid (EDTA) FeCl₂ and H₂O₂ (30%, w/v) used for peroxidation reaction were purchased from Merck (Darmstadt, Germany). The water was ultra-pure water obtained using a Milli-Q direct water purification system (Millipore, Billerica, MA, USA). All reagents were used without further purification

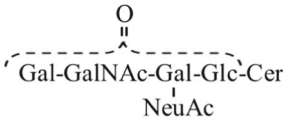
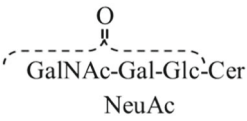
GM1 Oxidation by Fenton Reaction

Prior to oxidation, GM1 [GM1(d18:1/C18:0) and GM1(d20:1/C18:0)] were diluted to a final concentration of 1.0 mM using a mixture of CHCl₃/MeOH (1:1) and 30 μ L were transferred to a tube. Organic solvents were then dried under a nitrogen stream. Ammonium hydrogenocarbonate buffer 5 mM (pH 7.4) was added to the ganglioside, well homogenized for 10 min, placed in an ultrasonic water bath (Ultrasons; J.P. Selecta S.A., Barcelona, Spain) for 15 min, and homogenized again for 5 min until the formation of liposomes. Then, oxidation was initiated by adding FeCl₂ to a final concentration of 40 μ M, H₂O₂ to a final concentration of 50 mM and ethylenediaminetetraacetic acid (EDTA) to a final concentration of 40 μ M. The mixture was incubated in the dark at 37 °C, under orbital shaking at 500 rpm in a thermocycler up to 3 d. The reaction mixture was analyzed by mass spectrometry without prior purification. Identification of the oxidation products was done by LC-MS, ESI-MS, and MS/MS. The control experiments were performed using the same experimental procedure and by replacing H₂O₂, FeCl₂, and EDTA with ammonium hydrogenocarbonate 5 mM buffer.

Electrospray Mass Spectrometry and Tandem Mass Spectrometry Analysis in the Q Exactive Orbitrap

For elemental composition determination, the extent of GM1 oxidation and the identification of new products formed were monitored by ESI-MS on a Q Exactive hybrid quadrupole-Orbitrap mass spectrometer (Thermo Fisher Scientific, Bremen, Germany). The instrument was operated in negative-ion mode, with a spray voltage at 2.7 kV and interfaced with a H-ESI II ion source. Samples of non-oxidized and oxidized GM1 were diluted in pure MeOH, with a concentration of approximately 6 pmol. μ L⁻¹, and introduced through direct infusion at a flow rate of 5 μ L/min into the ESI source, and the operating conditions were as follows: sheath gas (nitrogen) flow rate 5 (arbitrary units); auxiliary gas (nitrogen) 1; capillary temperature 250 °C, S-lens rf level 50, and probe heater temperature 50 °C.

Table 1. Main Oxidation Products Observed in the High Resolution ESI-MS Spectra, Generated After Oxidation of GM1 Induced by the Hydroxyl Radical. Assignment of the m/z Values of the $[M - H]^-$ and $[M - 2H]^{2-}$ Molecular Ions, Proposed Structural Molecular and Their Most Probable Identification are Shown

	Proposed structural molecular	$[M-H]^-$	$[M-2H]^{2-}$
Oxidation products from GM1(d18:1/C18:0)	Gal-GalNAc-Gal-Glc-Cer NeuAc	1544.9	771.9
Oxygenated GM1 derivatives			
GM1+O-2Da		1558.8	778.9
GM1+O	Gal-GalNAc-Gal-Glc-Cer-NeuAc OH	1560.9	-
Oxidative cleavage of the glycan backbone and their oxidized derivatives			
asialo-GM1/(GM1-NeuAc _{res})	Gal-GalNAc-Gal-Glc-Cer	1253.8	-
GM2	GalNAc-Gal-Glc-Cer NeuAc	1382.8	690.9
GM2+O	GalNAc-Gal-Glc-Cer-NeuAc OH	1398.8	-
GM2+O-2Da		1396.8	697.9
asialo-GM2/(GM2-NeuAc _{res})	GalNAc-Gal-Glc-Cer	1091.7	-

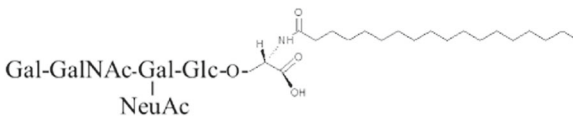
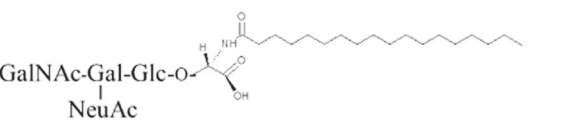
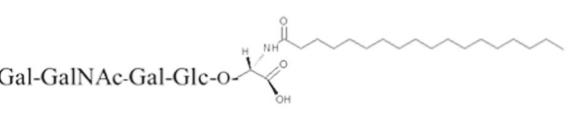
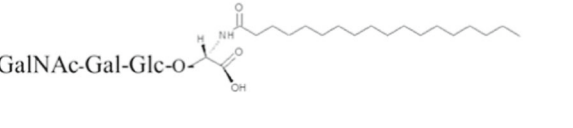
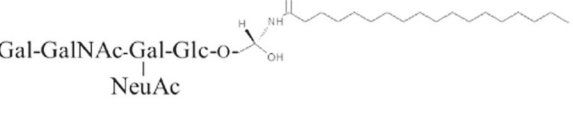
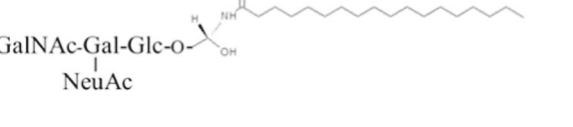
The acquisition method was set with a full scan and resolution was set to 140,000, the m/z ranges were set to 400–2000 in the normal mass range during full-scan experiments. The automatic gain control (AGC) target was set at 3×10^6 and the

maximum injection time (IT) was 100 ms. The Q Exactive system was tuned and calibrated in negative mode using peaks of known mass from a calibration solution (Thermo Scientific) to achieve a mass accuracy of <0.5 ppm RMS. Spectra were

Table 1. (continued)

GM3	Gal-Glc-Cer NeuAc	1179.7	589.4
LacCer/(GM3-NeuAc _{res})	Gal-Glc-Cer	888.6	-
GlcCer+O-2Da	$\begin{array}{c} \text{O} \\ \parallel \\ \text{GlcCer} \end{array}$	740.6	-
GlcCer	Glc-Cer	726.6	-
Cer	Cer	564.5	-
Cer+O-2Da	$\begin{array}{c} \text{O} \\ \parallel \\ \text{Cer} \end{array}$	578.5	-
Cer+O	$\begin{array}{c} \text{OH} \\ \\ \text{Cer} \end{array}$	580.5	-

**Oxidative cleavage of the
sphingosine backbone of
GM1**

C3-C4 cleavage		1350.6	674.8
C3-C4 cleavage -Hex _{res}		1188.6	593.8
C3-C4 cleavage - NeuAc _{res}		1059.5	-
C3-C4 cleavage -Hex _{res} - NeuAc _{res}		897.5	-
C2-C3 cleavage		1322.6	-
C2-C3 cleavage-Hex _{res}		1160.6	-

Glycans and oxidized**glycans**

Glycan	Gal-GalNAc-Gal-Glc NeuAc	997.3	-
Glycan-2Da	-	995.3	-
Glycan+O	Gal-GalNAc-Gal-O NeuAc	1013.3	506.2
Glycan-Hex _{res}	Gal-GalNAc-Gal NeuAc	835.3	-
Glycan-Hex _{res} -2Da	-	833.3	-
Glycan-Hex _{res} +O	Gal-GalNAc-O NeuAc	851.3	-

analyzed using the acquisition software Xcalibur ver. 3.0.63 (Thermo Scientific, San Jose, CA, USA).

In order to obtain the product ion spectra of the major components during ESI-MS experiments, the selected precursor ions were isolated by the quadrupole and sent to the higher energy collision dissociation (HCD) collision cell for fragmentation via the C-trap. In the MS/MS mode, the mass resolution of the Orbitrap analyzer was set at 70,000 full width at half maximum (FWHM), AGC target at 5×10^5 , maximum IT 120 ms, isolation window 1.0 m/z , and normalized collision energy (NCE) was manually optimized for every precursor to generate the most informative MS/MS spectra (between 25 to 35 arbitrary units).

High Performance Liquid Chromatography-Mass Spectrometry

The oxidized mixture of GM1 was separated by HPLC performed on a Waters Alliance 2690 HPLC system (Waters Corp., Milford, MA, USA) coupled to a linear ion trap mass spectrometer LXQ (Thermo Finnigan, San Jose, CA, USA). Mobile phase A consisted of water with 5% acetonitrile and 0.1% formic acid. Mobile phase B consisted of 99.9% acetonitrile, with 0.1% formic acid. Volumes of 5 μL of oxidized mixture (26 μg) diluted in 80% of mobile phase A (80 μL), were introduced into a Supelco Bio Wide Pore C5 column (15 $\text{cm} \times 0.5 \text{ mm}$, 5 μm). The mobile phase gradient was programmed as follows: initial conditions were 80% of A for

5 min; 5–20 min linear gradient to 50% of B; 20–40 min linear gradient to 100% of B held for 5 min; 45–55 min linear gradient to 80% of A held for 10 min. The flow rate through the column was 16 $\mu\text{L min}^{-1}$ and it was redirected to the linear ion trap mass spectrometer by a capillary (0.350 \times 0.150 mm) of 70 cm length using a home-made split. Just before entering in the mass spectrometer, MeOH with a flow rate of 10 $\mu\text{L min}^{-1}$ was added and mixed with the sample. The LXQ linear ion trap mass spectrometer (ThermoFinnigan, San Jose, CA, USA) was operated in negative-ion mode. Typical ESI conditions were as follows: a flow rate of 8 $\mu\text{L/min}$, electrospray voltage, 4.7 kV; capillary temperature, 275 $^\circ\text{C}$; and sheath gas flow, 25 units. An isolation width of 0.5 Da was used with a 30 ms activation time for MS/MS experiments. Full scan MS spectra and MS/MS spectra were acquired with a 50 and 200 ms maximum ionization time, respectively. Normalized collision energy TM (CE) was varied between 20 and 30 (arbitrary units) for MS/MS. Data acquisition was carried out on an Xcalibur data system (ver. 2.0).

Results

Nonenzymatic radical oxidation of GM1 was monitored by ESI-MS in negative-ion mode. This ganglioside has one sialic acid that is easily ionized, originating $[\text{M-H}]^-$ [28] and $[\text{M-2H}]^{2-}$ ions [29]. GM1 can also ionize as chloride adduct $[\text{M-H} + \text{Cl}]^{2-}$ [30]. The GM1 standard was composed by a mixture of two GM1 molecular species, 70% of GM1(d18:1/

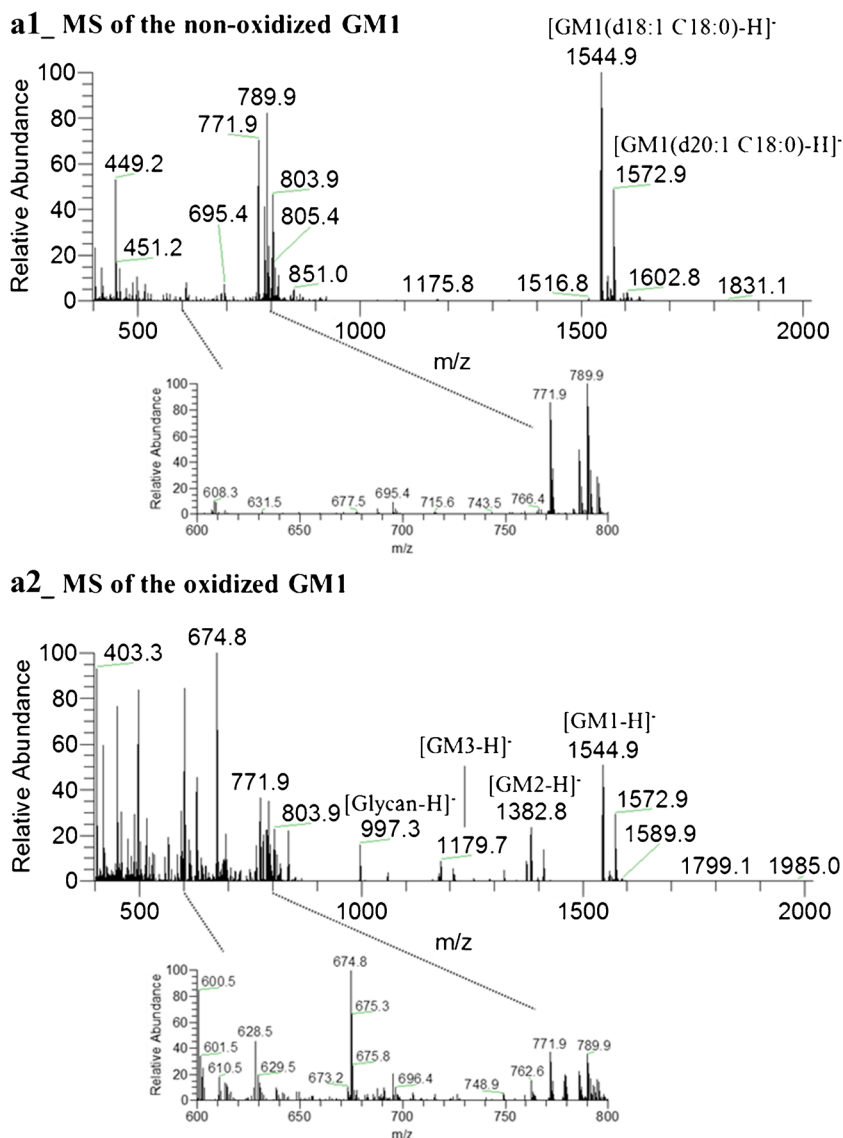


Figure 1. Oxidation of GM1 induced by the hydroxyl radical and monitored by ESI-MS. Comparison of the high resolution ESI mass spectrum of non-oxidized GM1 (**a1**), and oxidized GM1 (**a2**). Oxidation was induced by the hydroxyl radical produced upon Fenton reaction ($\text{H}_2\text{O}_2/\text{Fe}^{2+}$)

C18:0) (Neu5Ac α 2-3(Gal β 1-3GalNAc β 1-4)Gal β 1-4Glc- β 1Cer) and 30% of GM1(d20:1/C18:0), (Supplementary Figure S1), which we could not efficiently isolate.

The ESI-MS spectrum of the oxidized GM1 mixture (GM1/ Fe^{2+} / H_2O_2) showed several previously unobserved ions (Figure 1 and Supplementary Table S1), with higher and lower m/z values compared with non-oxidized ganglioside. In the MS spectrum, it is possible to observe the equivalent oxidation products for both GM1 molecular species, so our discussion will focus on reviewing the oxidation products from the most abundant molecular species of GM1 (i.e., the GM1(d18:1/C18:0)). This molecular species was observed at m/z 1544.9 and 771.9, assigned as $[\text{M}-\text{H}]^-$ and $[\text{M}-2\text{H}]^{2-}$ ions, respectively. Oxidation products with higher molecular weight, compared with GM1(d18:1/C18:0), were detected as $[\text{M}-\text{H}]^-$ at m/z

1558.8 and 1560.9, and assigned as keto (+14 Da) and hydroxy derivatives (+16 Da), respectively (Table 1). The keto derivatives molecular ions were also observed as $[\text{M}-2\text{H}]^{2-}$ at m/z 778.9.

On the other hand, abundant ions with m/z values lower than that of GM1 also were observed and assigned as products formed due to oxidative cleavage of glycosidic bonds of glycan chain of GM1. The glycan oxidative cleavage led to formation of GM2 ($[\text{M}-\text{H}]^-$ at m/z 1382.8), GM3 ($[\text{M}-\text{H}]^-$ at m/z 1179.7), and less abundant ions, assigned as asialo-GM1 (GM1-NeuAc $_{\text{res}}$; $[\text{M}-\text{H}]^-$ at m/z 1253.8), asialo-GM2 (GM2-NeuAc $_{\text{res}}$; $[\text{M}-\text{H}]^-$ at m/z 1091.7), LacCer ($[\text{M}-\text{H}]^-$ at m/z 888.6), and GlcCer ($[\text{M}-\text{H}]^-$ at m/z 726.6) (Supplementary Figure 1 and Table 1). GM2 and GM3 were also seen as $[\text{M}-2\text{H}]^{2-}$. Low abundant ions of oxidized GM2, as keto and hydroxy derivatives were observed as $[\text{M}-\text{H}]^-$ ions

Table 2. Accurate Mass Measurements of the New Ions Detected by MS After Oxidation. All Ions are Assigned with Their Predicted Formula, Observed Mass, Calculated Mass, and Mass Error

Oxidation Products	Predicted formula	Observed mass (Da)	Calculated mass (Da)	Error (mDa)	Error (ppm)
From GM1(d18:1/C18:0) oxidation					
[M – H] [–]					
GM1(d18:1/C18:0) + O	C ₇₃ H ₁₃₀ N ₃ O ₃₂	1560.862	1560.8643	2.3	1.5
GM1(d18:1/C18:0) + O-2 Da	C ₇₃ H ₁₂₈ N ₃ O ₃₂	1558.8464	1558.8486	2.2	1.4
GM1(d18:1/C18:0)	C ₇₃ H ₁₃₀ N ₃ O ₃₁	1544.8694	1544.8694	0	0.0
GM2(d18:1/C18:0) + O	C ₆₇ H ₁₂₀ N ₃ O ₂₇	1398.8095	1398.8115	2	1.4
GM2(d18:1/C18:0) + O-2 Da	C ₆₇ H ₁₁₈ N ₃ O ₂₇	1396.7959	1396.7958	–0.1	–0.1
GM2(d18:1/C18:0)	C ₆₇ H ₁₂₀ N ₃ O ₂₆	1382.8149	1382.8166	1.7	1.2
AsialoGM1(d18:1/C18:0)	C ₆₂ H ₁₁₃ N ₂ O ₂₃	1253.7729	1253.774	1.1	0.9
GM3(d18:1/C18:0)	C ₅₉ H ₁₀₇ N ₂ O ₂₁	1179.736	1179.7372	1.2	1.0
AsialoGM2(d18:1/C18:0)	C ₅₆ H ₁₀₃ N ₂ O ₁₈	1091.7199	1091.7211	1.2	1.1
LacCer(d18:1/C18:0)	C ₄₈ H ₉₀ NO ₁₃	888.6432	888.6418	–1.4	–1.6
GlcCer(d18:1/C18:0) + O-2 Da	C ₄₂ H ₇₈ NO ₉	740.5686	740.5682	–0.4	–0.5
GlcCer(d18:1/C18:0)	C ₄₂ H ₈₀ NO ₈	726.5893	726.5889	–0.4	–0.6
Cer(d18:1/c18:0) + O	C ₃₆ H ₇₀ NO ₄	580.5309	580.531	0.1	0.2
Cer(d18:1/c18:0) + O-2 Da	C ₃₆ H ₆₈ NO ₄	578.5173	578.5154	–1.9	–3.3
Cer(d18:1/c18:0)	C ₃₆ H ₇₀ NO ₃	564.5379	564.5361	–1.8	–3.2
C3-C4 cleavage	C ₅₈ H ₁₀₀ N ₃ O ₃₂	1350.6259	1350.6295	3.6	2.7
C2-C3 cleavage	C ₅₇ H ₁₀₀ N ₃ O ₃₁	1322.6331	1322.6346	1.5	1.1
C3-C4 cleavage-Hex _{res}	C ₅₂ H ₉₀ N ₃ O ₂₇	1188.5745	1188.5767	2.2	1.9
C2-C3 cleavage-Hex _{res}	C ₅₁ H ₉₀ N ₃ O ₂₆	1160.581	1160.5818	0.8	0.7
C3-C4 cleavage-NeuAc _{res}	C ₄₇ H ₈₃ N ₂ O ₂₄	1059.5334	1059.5341	0.7	0.7
Glycan + O	C ₃₇ H ₆₁ N ₂ O ₃₀	1013.3287	1013.3315	2.8	2.8
Glycan	C ₃₇ H ₆₁ N ₂ O ₂₉	997.3355	997.3365	1	1.0
Glycan-2 Da	C ₃₇ H ₅₉ N ₂ O ₂₉	995.3167	995.3209	4.2	4.2
Glycan-Hex _{res} + O	C ₃₁ H ₅₁ N ₂ O ₂₅	851.2748	851.2786	3.8	4.5
Glycan-Hex _{res}	C ₃₁ H ₅₁ N ₂ O ₂₄	835.2837	835.2837	0	0.0
Glycan-Hex _{res} -2 Da	C ₃₁ H ₄₉ N ₂ O ₂₄	833.2653	833.2681	2.8	3.4
[M + Na – 2H] [–]				0	
C3-C4 cleavage	C ₅₈ H ₉₉ N ₃ NaO ₃₂	1372.6099	1372.6115	1.6	1.2
C3-C4 cleavage-Hex _{res}	C ₅₂ H ₈₉ N ₃ NaO ₂₇	1210.5578	1210.5587	0.9	0.7
[M + Na-3H] ^{2–}				0	
C3-C4 cleavage	C ₅₈ H ₉₈ N ₃ NaO ₃₂	685.803	685.8021	–0.9	–1.3
[M – 2H] ^{2–}				0	
C3-C4 cleavage	C ₅₈ H ₉₉ N ₃ O ₃₂	674.8119	674.8111	–0.8	–1.2
C3-C4 cleavage-Hex _{res}	C ₅₂ H ₈₉ N ₃ O ₂₇	593.7826	593.7847	2.1	3.5
GM1(d18:1/C18:0) + O-2 Da	C ₇₃ H ₁₂₇ N ₃ O ₃₂	778.9204	778.9207	0.3	0.4
GM1(d18:1/C18:0)	C ₇₃ H ₁₂₉ N ₃ O ₃₁	771.9311	771.9311	0	0.0
GM2(d18:1/C18:0)	C ₆₇ H ₁₁₉ N ₃ O ₂₆	690.9053	690.9047	–0.6	–0.9
GM3(d18:1/C18:0)	C ₅₉ H ₁₀₆ N ₂ O ₂₁	589.3667	589.365	–1.7	–2.9
Glycan + O	C ₃₇ H ₆₀ N ₂ O ₃₀	506.16	506.1621	2.1	4.1
[M + Cl] [–]				0	
AsialoGM1(d18:1/C18:0) + Cl ³⁵	C ₆₂ H ₁₁₄ Cl ³⁵ N ₂ O ₂₃	1289.7485	1289.7506	2.1	1.6
Cer(d18:1/c18:0) + O + Cl ³⁵	C ₃₆ H ₇₁ Cl ³⁵ NO ₄	616.5092	616.5077	–1.5	–2.4
Cer(d18:1/c18:0) + Cl ³⁵	C ₃₆ H ₇₁ Cl ³⁵ NO ₃	600.5145	600.5128	–1.7	–2.8
Cer(d18:1/c18:0) + O-2 Da + Cl ³⁵	C ₃₆ H ₆₉ Cl ³⁵ NO ₄	614.4934	614.4921	–1.3	–2.1
[M + Cl-H] ^{2–}				0	
GM1(d18:1/C18:0) + Cl ³⁵ -H	C ₇₃ H ₁₃₀ Cl ³⁵ N ₃ O ₃₁	789.9198	789.9194	–0.4	–0.5
GM2(d18:1/C18:0) + Cl ³⁵ -H	C ₆₇ H ₁₂₀ Cl ³⁵ N ₃ O ₂₆	708.8935	708.893	–0.5	–0.7

at m/z 1396.8 and 1398.8, respectively. Keto derivatives of GlcCer were observed at m/z 740.6. Nonenzymatic oxidative cleavage between Cer and glycan led to the release of free glycans ([glycan-H][–], observed at m/z 997.3, and [glycan-Hex_{res}-H][–], observed at m/z 835.3), as well as ceramide ([Cer-H][–] observed at m/z 564.5) (Supplementary Figure 1 and Table 1). Their oxidized counterparts were also detected in the MS spectrum, namely Glycan-2 Da, Glycan + O, Glycan-Hex_{res}-2 Da, Glycan-Hex_{res} + O, Cer + O-2 Da, and Cer + O (Table 1). Oxidative cleavages of glycan backbone were observed during oxidation of oligosaccharides and of lactosylceramide, whereas oxidative cleavages between Cer

and glycan under nonenzymatic condition have been reported to occur by oxidation of lactosylceramide and galactosylceramide [24, 31, 32].

Furthermore, in the ESI-MS spectrum of oxidized GM1, it was possible to observe new ions due to oxidative cleavage of GM1 sphingosine backbone between C3 and C4 with formation of –COOH terminal in C3 ([M-H][–] at m/z 1350.6 and [M-H]^{2–} at m/z 674.8), between C2 and C3 with formation of a terminal –CH₂OH in C2 (as [M-H][–] at m/z 1322.6) (Table 1). Also, oxidative cleavage of sphingosine backbone between C3 and C4 was observed for GM2, asialo-GM1, and asialo-GM2, and between C2 and C3 for GM2 (Table 1). The proposed

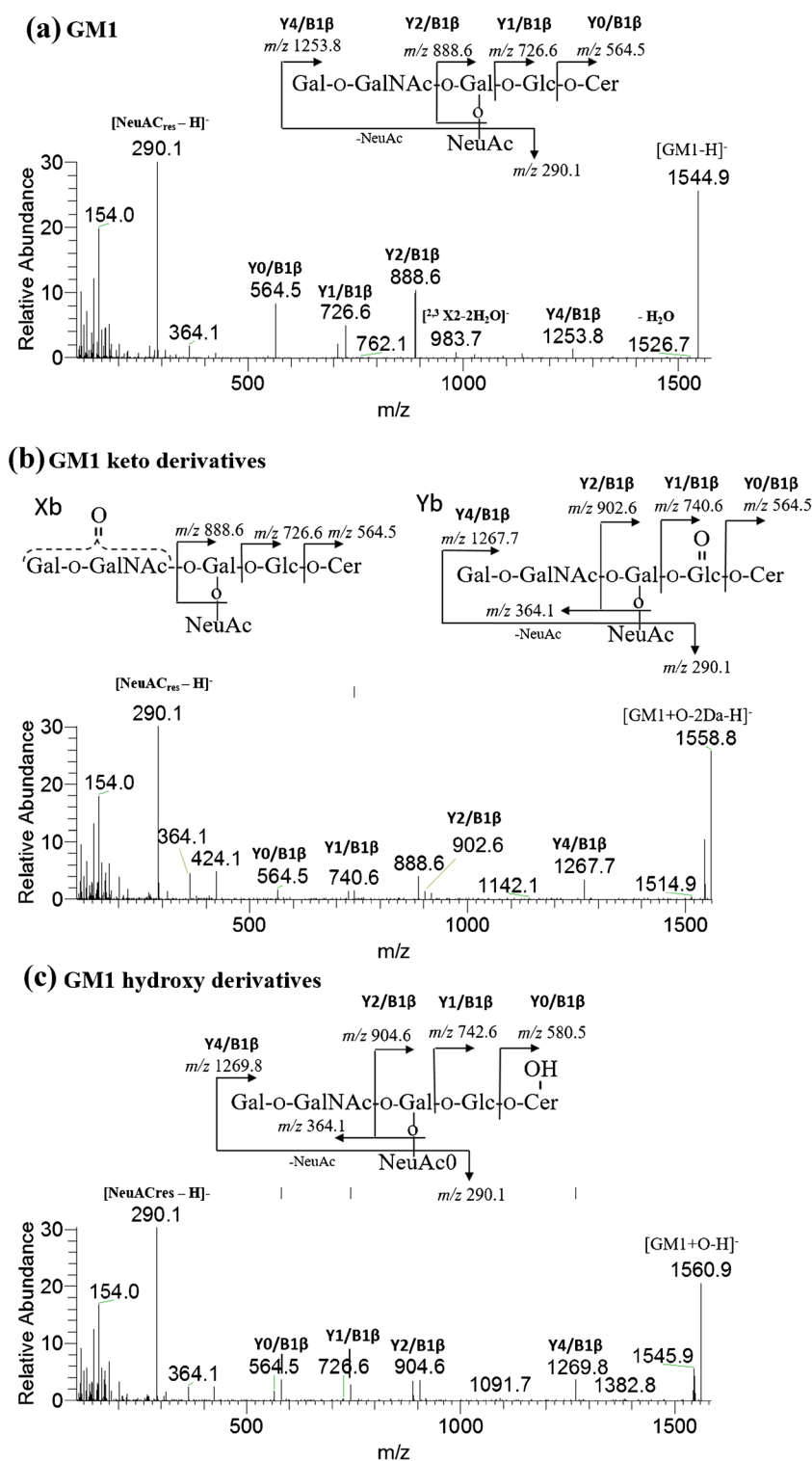


Figure 2. MS/MS spectra of non-modified GM1 and of oxygenated GM1 derivatives. High resolution MS/MS spectrum of the GM1, assigned as [GM1 – H]⁻ at m/z 1544.9 and their fragmentation pathways (a); MS/MS spectrum of the keto derivatives, observed at m/z 1558.8. Three possible positional isomers in the carbohydrate chain are possible: structures with a keto group in Gal (IV) and/or GalNAc (III) residues (b-xb) and in Glc (I) residue (b-yb) (b); MS/MS spectrum of the hydroxy derivatives of GM1, assigned as [GM1 + O-H]⁻, at m/z 1560.9 and their fragmentation pathways when the hydroxy group is present in the ceramide moiety (c)

molecular composition of all these oxidation products was corroborated by performing exact mass measurements through high resolution Orbitrap mass spectrometry (Table 2).

The presence of isomeric oxidation products was investigated by analyzing the oxidized GM1 sample by RP-HPLC-MS, as described in Experimental section. The reconstructed

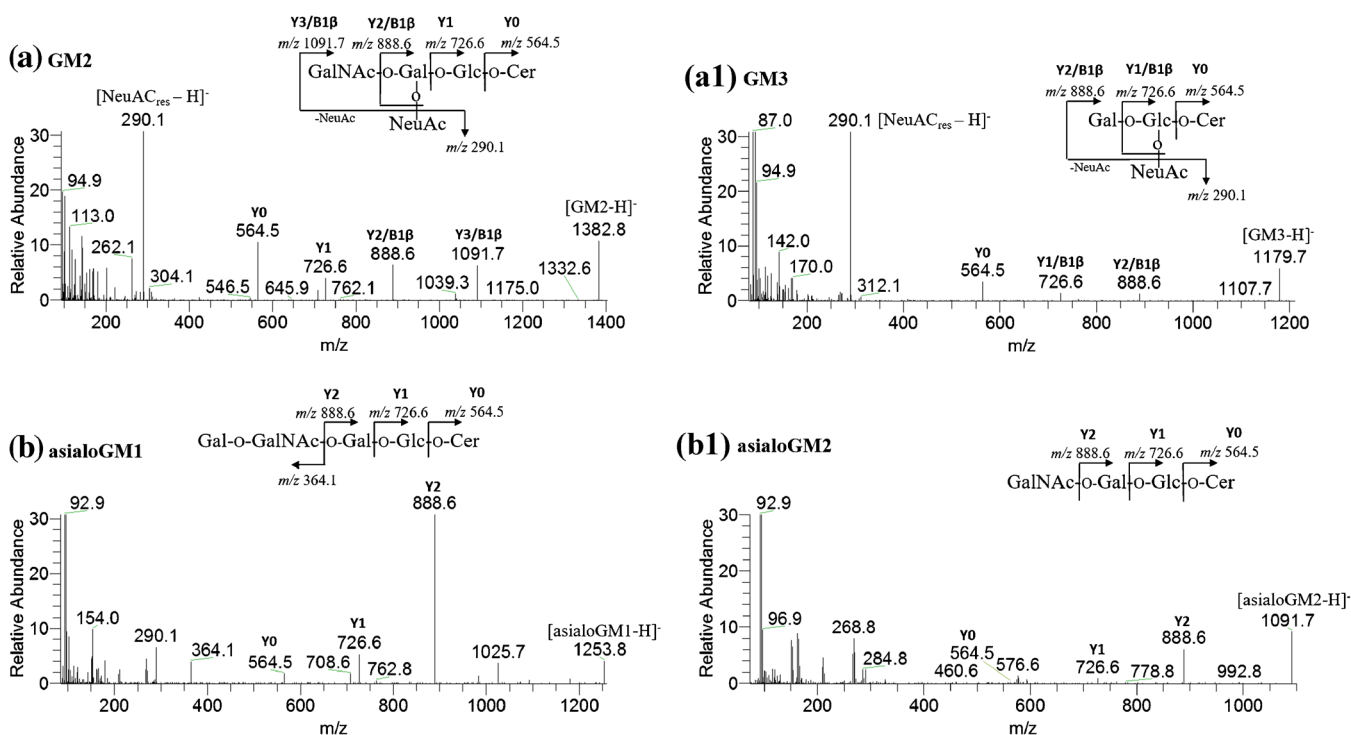


Figure 3. MS/MS spectra of the new gangliosides formed due to oxidative cleavage of carbohydrate chain of GM1. High resolution MS/MS spectra of asialo-GM1 (GM1- NeuAc_{res}) (**a2**), GM2 (**b1**) asialo-GM2 (GM2-NeuAc_{res}) (**b2**), GM3 (**c1**)

ion chromatograms (RICs) of the [GM1 (d18:1/C18:0)-H]⁻, [GM1(d18:1/C18:0) + O-2 Da-H]⁻, [GM1(d18:1/C18:0) + O-H]⁻, [GM2(d18:1/C18:0)-H]⁻, [GM1(d3^{COOH}/C18:0)-H]⁻, [GM1(d2^{CH₂OH}/C18:0)-H]⁻, [Glycan-H]⁻, [Glycan-Hex_{res}-H]⁻ molecular ions showed that each of these oxidized species eluted in only one peak, suggesting the absence of structural isomeric species (Supplementary Figure S3).

Tandem Mass Spectrometry Analysis of Oxidized GM1

ESI-MS/MS analysis corroborated the previous assigned modifications of GM1. The fragmentation pathways observed for the [M-H]⁻ of non-modified GM1 (Figure 2a and Supplementary Figure S2a), observed at *m/z* 1544.7, involved the typical loss of NeuAc_{res} (-291 Da) (*m/z* 1253.8) and diagnostic ions [LacCer-H]⁻ (*m/z* 888.6), [GlcCer-H]⁻ (*m/z* 726.6), and [Cer-H]⁻ (*m/z* 564.5) as previously reported [28]. On the other hand, the MS/MS spectrum of the [M-2H]²⁻ molecular ion exhibits other informative product ions assigned as the unaltered fatty acyl chain (*m/z* 308.3) [33], and glycan ions such as [glycan-H]⁻ ion at *m/z* 997.3, [glycan-Hex_{res}-H]⁻ at *m/z* 835.3, [HexGalNAc_{res}-H]⁻ at *m/z* 364.1, [NeuAc_{res}-H]⁻ at *m/z* 290.1, [GalNAc_{res}-H]⁻ at *m/z* 202.1, [Hex_{res}-H]⁻ at *m/z* 179.1 (Supplementary Figure S3b) [30, 34]. Shifts in these typical ions were used to identify oxidative modifications and structural features of the products formed during the radical oxidation of GM1.

The ESI-MS/MS spectra of the [M-H]⁻ ions of the oxygenated GM1, namely GM1 keto (GM1 + O-2 Da; *m/z* 1558.8) (Figure 2b and Supplementary Figure S2c) and hydroxy (GM1

+ O; *m/z* 1560.9) (Figure 2c and d) derivatives (Supplementary Table S2), showed product ions corresponding to a non-modified neutral loss of NeuAc_{res} (-291 Da), oxidized LacCer (assigned as [LacCer + O-2 Da-H]⁻ or [LacCer + O-H]⁻) and oxidized GlcCer (assigned as [GlcCer + O-2 Da-H]⁻ or [GlcCer + O-H]⁻), respectively, (Figure 2 and Supplementary Figure S2). The presence of oxidized Cer was inferred by the presence of the product ion at *m/z* 580.5, attributed to [Cer + O-H]⁻. This indicated that hydroxyl group in GM1 hydroxy derivative is located in Cer.

In GM1 keto derivative, the absence of oxidized Cer and the presence of [Cer-H]⁻ ion suggest that oxidation occurs in glycan moiety. In the MS/MS spectrum of GM1 keto derivative (Figure 2b and Supplementary Figure S2c), the [LacCer + O-2 Da-H]⁻ product ion (*m/z* 902.6) indicate that the oxidation has occurred in the glucose (I) (Glc) or galactose (II) (Gal) residues. The observation of the [GlcCer + O-2 Da-H]⁻ product ion (*m/z* 740.6) corroborated oxidation in Glc (I). In this case, the loss of 2 Da occurs, most probably, from the formation of a keto group on the sugar moiety. On the other hand, the presence of [LacCer-H]⁻ product ion (*m/z* 888.6) suggests oxidation in another Gal (IV) or *N*-acetylgalactosamina (III) (GalNAc).

The formation of new gangliosides from GM1, under non-enzymatic oxidation conditions, was confirmed by tandem mass spectrometry (Figure 3 and Supplementary Figures S4, S5, and Supplementary Table S3). These new gangliosides include GM2, GM3, asialo-GM1, asialo-GM2, the globoside LacCer (GM3-NeuAc_{res}), and the cerebroside GlcCer, arising from oxidative depolymerization of GM1. The ESI-MS/MS

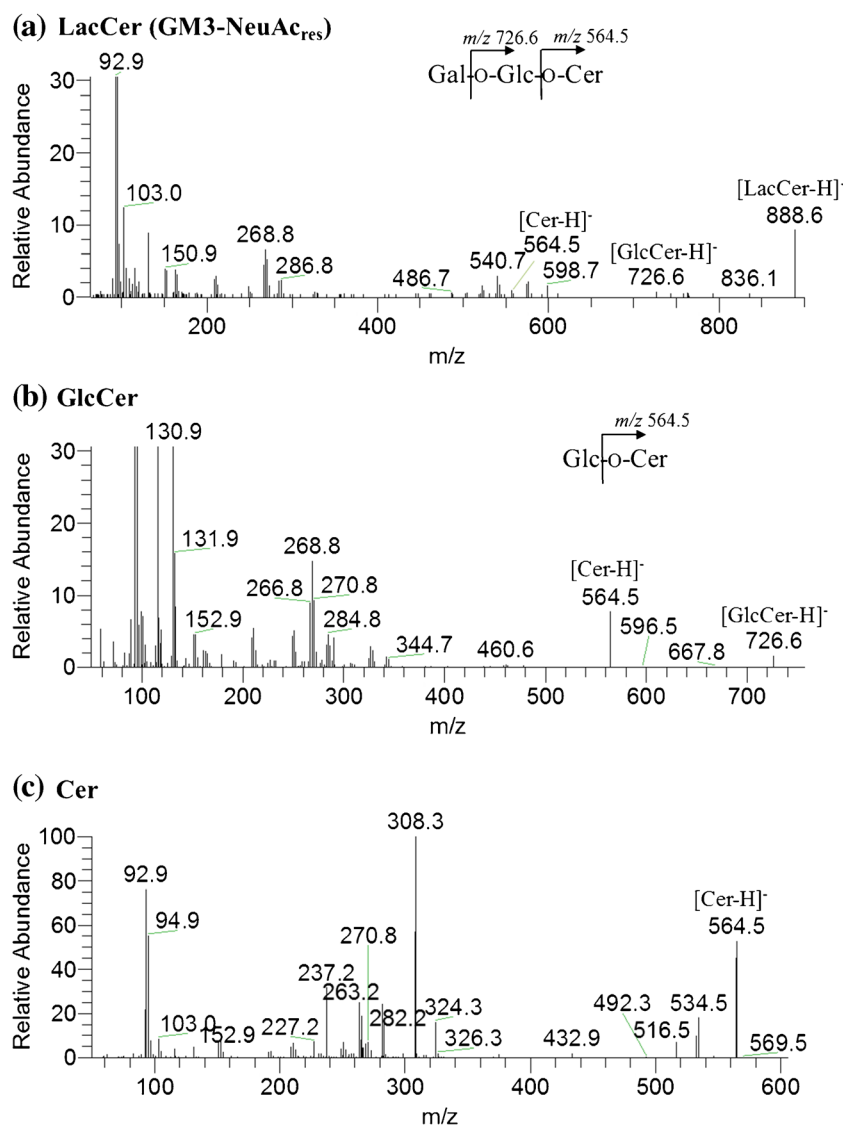


Figure 4. MS/MS spectra of the new glycosphingolipids and Ceramide formed due to oxidative cleavage of GM1. High resolution MS/MS spectra of LacCer (GM3-NeuAc_{res}) (a), GlcCer (b), and Cer (c)

spectra of the asialo-GM1, GM2, and GM3 showed product ion characteristics of the fragmentation pathways previously reported for these gangliosides [28, 34]. In all MS/MS spectra (asialo-GM1, Figure 3b; GM2, Figure 3a; asialo-GM2, Figure 3b1; GM3, Figure 3a1), LacCer Figure 4a; and GlcCer, Figure 4b and Supplementary Figure S5) it was possible to observe the non-modified ceramide product ion (m/z 564.5), confirming the presence of ceramide (d18:1/C18:0). Additionally, the MS/MS spectra of the GM2 and GM3 also showed two abundant product ions, one arising from the characteristic neutral loss of NeuAc_{res} (-291 Da) and the product ion at m/z 290.1, assigned as [NeuAc_{res}-H]⁻. These product ions were not observed in the MS/MS spectra of asialogangliosides, LacCer and GlcCer (Figure 4 and Supplementary Figure S5).

The oxidation of GM1 under Fenton conditions also led to the formation of un-oxidized ceramides and un-oxidized and oxidized glycans. The ESI-MS/MS spectrum of un-oxidized ceramide (m/z 564.5) generated from oxidation of GM1 was

obtained and fragmentation pathways yielded product ions at m/z 324.3, 308.3, 282.2, 265.3, 263.2, and 237.2, which were assigned to be S, T, U, V, R, and P ions, respectively, as previously reported (Figure 4c [33, 35]). These data confirmed the release of ceramides during nonenzymatic radical oxidation of GM1. Similar results were observed in previous experiments, during the radical oxidation of GalCer and LacCer [24].

The MS/MS spectrum of the molecular ions observed at m/z 997.3, identified as [Glycan-H]⁻, and at m/z 835.3, identified as [Glycan-Hex_{res}-H]⁻, showed typical product ions that arose from glycosidic bond cleavages (product ions of non-modified glycosidic moieties at m/z 364.1 and 290.1) and cross-ring cleavages arising from neutral loss of 120 Da [product ions observed at m/z 586.2 (glycan-120 Da-NeuAc_{res}) and 424.1 (glycan-hex_{res}-120 Da-NeuAc_{res})] (Supplementary Table S4). Additionally, and as expected, [Cer-H]⁻ product ions were not observed. The MS/MS analysis of oxidized glycans molecular ions,

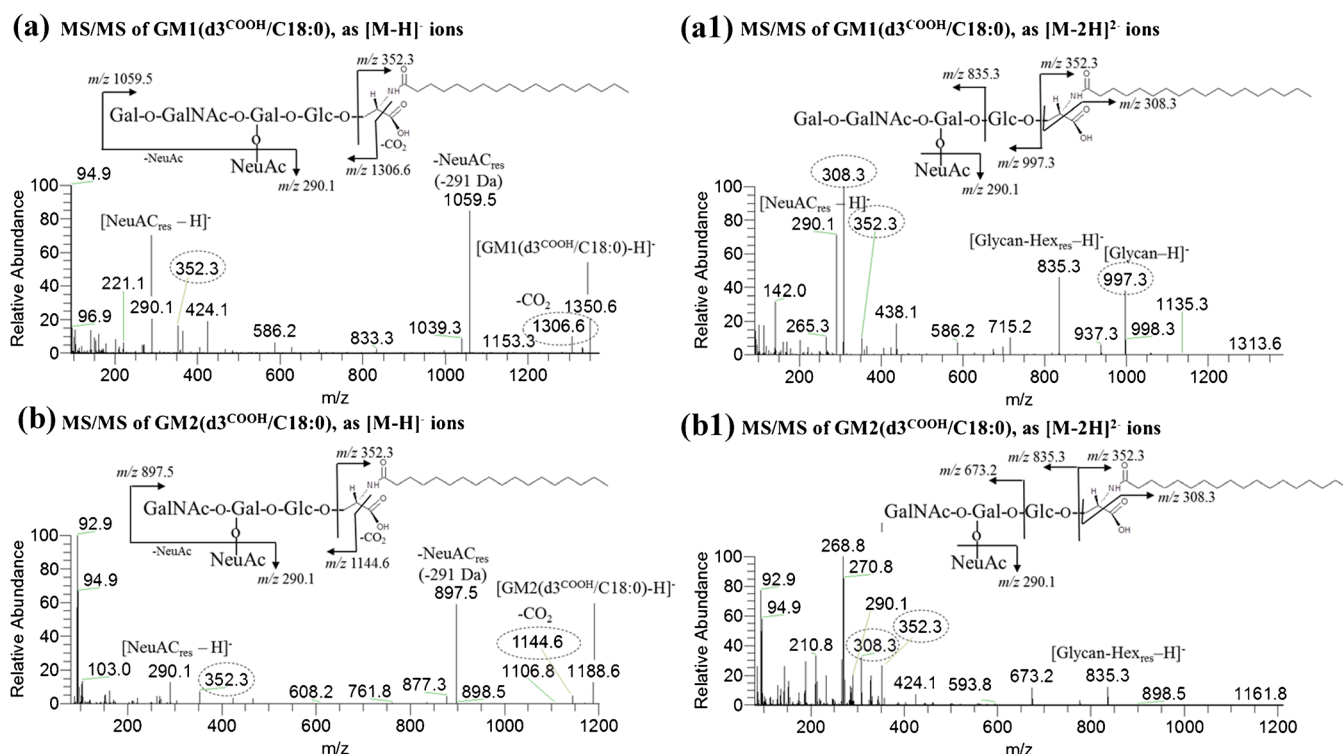


Figure 5. MS/MS spectra of products formed due to oxidative cleavage between C3 and C4 of sphingosine backbone of GM1 and GM2. High resolution MS/MS spectra of GM1 derivatives assigned as $[GM1(d3^{COOH}/C18:0)-H]^-$ singly charged ion (a) and $[GM1(d3^{COOH}/C18:0)-2H]^{2-}$ doubly charged ion (a1). MS/MS spectra of GM2 derivatives assigned as $[GM2(d3^{COOH}/C18:0)-H]^-$ singly charged ion (b) and $[GM2(d3^{COOH}/C18:0)-2H]^{2-}$ doubly charged ion (b1)

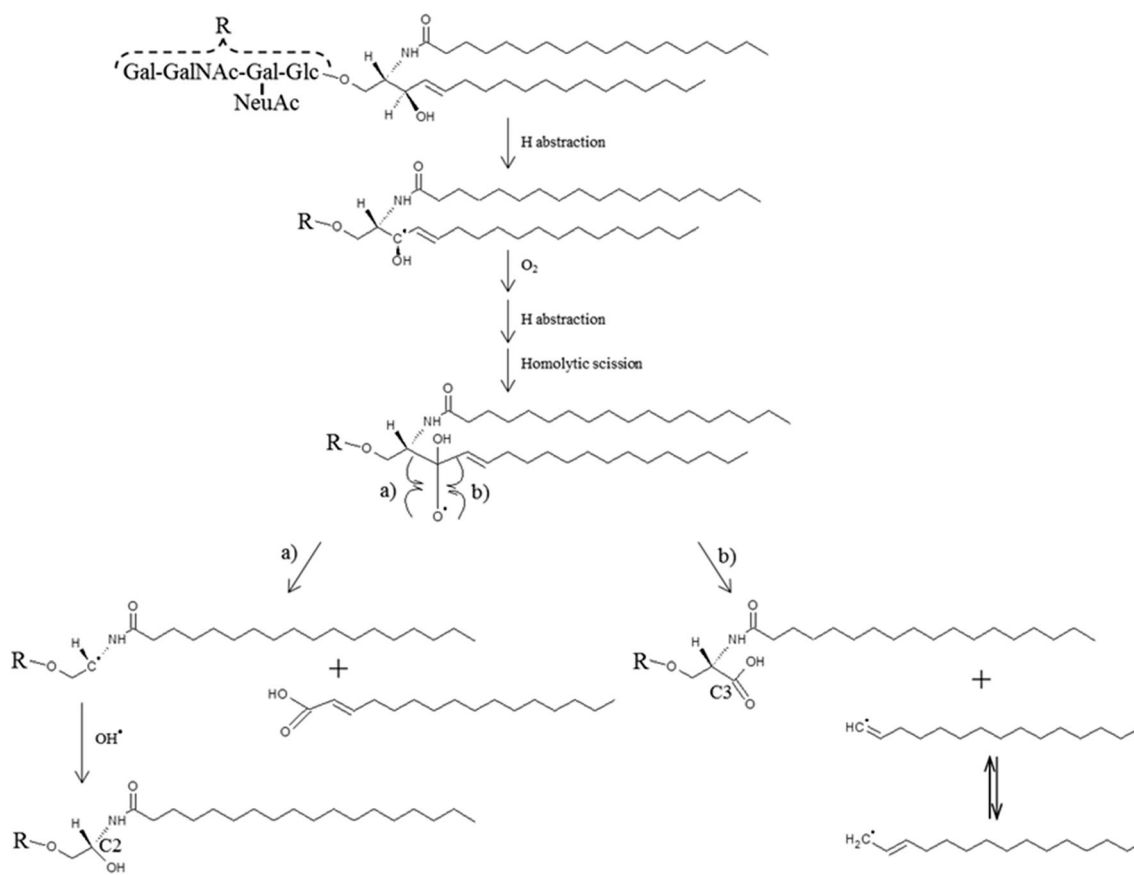
arising from nonenzymatic oxidation of GM1, at m/z 1013.3, assigned as $[glycan + O-H]^-$ and at m/z 851.3, assigned as $[glycan-Hex_{res} + O-H]^-$ showed the neutral loss of $NeuAc_{res}$ (-291) and a product ion arising from the neutral loss of CO_2 (-44 Da) (Supplementary Figure S6), which was not observed in non-modified glycan. This suggests the formation of a new carboxylic acid group (-COOH) in the chain. These oxidized glycans can be generated after the release of glycan and, most probably, the oxidation occurs at C1 of the reducing end sugar unit, with formation of hexonic acid, as suggested for oligosaccharides under radical oxidation [31].

Based on the accurate mass measurement information and analysis of MS/MS spectra, the oxidation products observed in the MS spectra of oxidized GM1 at m/z 1350.6, 1188.6 were assigned as species arising from oxidative cleavage of the sphingosine backbone at C3-C4, with formation of a -COOH terminal group. Also, the oxidation products observed at m/z 1313.6, 1161.8 were assigned as species arising from the oxidative cleavage of the sphingosine backbone at C2-C3, with formation of a -CH₂OH terminal group. The tandem mass spectra of these ions were analyzed, allowing the confirmation of the proposed structures. The MS/MS spectra of the $[M-H]^-$ ion of the molecular ion arising from C3-C4 cleavage of GM1 and GM2 showed fragment ions arising from neutral loss of CO_2 (-44 Da), confirming the terminal carboxylic acid. The abundant product ion arising from a neutral loss of 291 Da

observed in both MS/MS spectra, and the absence of Cer, GluCer, and LacCer fragment ions, as well as the presence of fragment ions corresponding to non-modified sugars (as described above), reinforce the existence of modified Cer moiety (Figure 5a and b, and Supplementary Table S5). The product ion at m/z 352.3 arising from loss of non-modified glycan backbone (-998 Da or -836 Da from oxidized GM1 or GM2 ion, respectively), confirmed the cleavage of C3-C4 bond of sphingosine backbone (Figure 5a and b, and Supplementary Table S5). The MS/MS of the doubly charged molecular ions confirmed the attribution to non-modified glycan backbone, corroborated by the presence of the product ions at m/z 997.3 (for oxidized GM1 derivative) and 835.3 (for oxidized GM2 derivative). Furthermore, the presence of unmodified fatty acyl chain was corroborated by the presence of the product ion at m/z 308.3 (Figure 5a1 and b1). The MS/MS spectrum of the molecular ion arising from C3-C4 cleavage of asialo-GM1, observed at m/z 1059.5, did not provide any additional information but shared the same diagnostic ion at m/z 352.3 that corroborated the proposed structure (Supplementary Table S5).

Discussion

This study demonstrated that the oxidation of gangliosides by hydroxyl radical generated by Fenton reaction leads to the formation of a wide variety of oxidation products, with



Scheme 1. Mechanism proposed for the formation of ions observed in the high resolution ESI-MS spectrum, arising from the cleavage of C2-C3 (a) and C3-C4 (b) of sphingosine backbone

different structural features. In this work, we used liposomes with pure glycolipids and higher concentration of H₂O₂ than the physiologic conditions as models of lipid oxidation. The objective has been to obtain an unequivocal molecular characterization of the different products formed during oxidation. This information is indispensable for its unambiguous detection in biological matrices, and to develop targeted lipidomic methods for their sensitive detection *in vivo*.

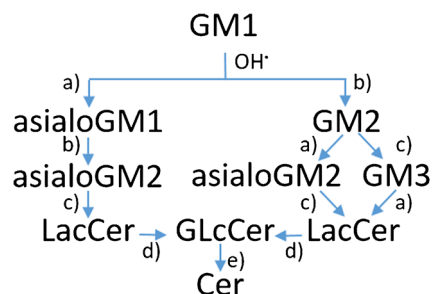
Nonenzymatic oxidation of GM1 generates oxygenated GM1 as keto and hydroxy derivatives and oxidation products derived from oxidative cleavage of sphingosine and also of the glycan chain. Sphingosine oxidation seems to occur after abstraction of one hydrogen from C3, with subsequent fragmentation between C2 and C3 (with formation of a hydroxyl group in C2) and C3-C4 (with formation of a carboxylic acid group in C3) of sphingosine backbone (Scheme 1).

The *in vitro* GM1 oxidation leads to the formation of smaller gangliosides, namely GM2, GM3, asialo-GM1, and asialo-GM2, oxygenated GM2 (as keto and hydroxy derivatives), and other glycolipids: LacCer, GlcCer, hydroxyl-GlcCer, ceramide, keto, and hydroxy derivatives of Cer and glycans, oxidized glycans (assigned glycans-2 Da) were also formed in these oxidative conditions (Scheme 2).

The reaction of the hydroxyl radicals with GSLs may yield different carbon-centered radicals. The formation of these products can occur as a result of formation of C1 and C2

radicals in hexoses, like previously reported for oxidation of GalCer by radiation [23]. Additionally, cleavage of the glycosidic bonds of GM1 with centered radicals in C2 can afford the formation of species aforementioned, except the formation of glycans [23, 36].

Gangliosides are glycosphingolipids containing a sialic acid and they are quite abundant in nervous system. Over 90% of the total ganglioside content of the adult brain is comprised of the four complex ganglioside species, GM1a, GD1a, GD1b, and GT1b [37]. GM3 and GD3 are precursors of these more



Scheme 2. The formation of new gangliosides, glycosphingolipids and ceramides through nonenzymatic degradation of GM1. Products formed due to oxidative cleavage of carbohydrate chain of the GM1 by hydroxyl radical, generated by Fenton reaction. (a) -NeuAc_{res}, (b) -Gal_{res} (IV), (c) -GalNAc_{res} (III), (d) -Gal_{res} (II), (e) -Glc_{res} (I)

complex gangliosides, as reviewed in [38, 39]. Gangliosides are highly expressed in the plasma membrane of neurons and are particularly important for neurons development, regulating axonal growth, signaling, and repair, and are important for the myelin stability and nerve regeneration by binding to a specific myelin-associated glycoprotein. Changes in ganglioside composition and content have been associated with several neurodegenerative diseases and age mental disorders, which are associated with increased oxidative stress and ROS production [17]. However, the expression patterns of the GM1 and GD1a suggested that these degradation pathways can be more complex [40]. Changes in the concentration of gangliosides were observed in neurodegenerative diseases. In some regions of the CNS of Alzheimer's disease patients, a decrease in the concentration of GT1b, GD1b, GD1a, and GM1 from the complex ganglio-series gangliosides was observed, and an increase in concentration of "simple" gangliosides, such as GM2, GM3, and GM4 occurs [13]. In amyotrophic lateral sclerosis patients, another neurodegenerative disease, an increase in the concentrations of the GM2 and GD3 (simple gangliosides) was also observed [14]. Recent studies suggested that the accumulation of simple gangliosides in AD is a result of the cleavage of the more complex of the series A gangliosides by enzymatic degradation pathways [40]. However, the expression patterns of the GM1 and GD1a suggested that these degradation pathways can be more complex [40]. In this context, considering our results, it can be suggested that under oxidative stress conditions, more complex gangliosides that are essential for the brain development and function, such as GM1, may suffer degradation by oxidative process. These processes are typically associated with age-associated neurodegenerative diseases, such as AD and PD [12–15]. Thereby, both enzymatic degradation and oxidative stress can be contributing for the accumulation of simple gangliosides, through the degradation of more complex species. This latter process might cause a disruption of the typical profile of gangliosides in neurons, and could be associated with neuronal dysfunction.

In this study, the release of ceramides due to oxidative degradation of GM1 was also observed. Like for some gangliosides, in the brains of subjects with Alzheimer's disease and other neurodegenerative diseases, variations in the concentration of ceramides, more specifically an increase were observed [41]. Our results are in agreement with a previous study showing that the accumulation of ceramides, present in neurons of AD, occurs with oxidative stress, even though it was suggested to be only due to alterations in enzymatic pathways [42]. More recently, it was also reported that glycosphingolipids, under distinct oxidation conditions, lead to formation of ceramides [23, 24, 43]. Ceramides are pro-apoptotic agents and participate in the neuronal cell death that leads to Alzheimer's disease (AD) [44].

This study provides a new perspective regarding the putative contribution of radical oxidative induced depolymerization of gangliosides, which can be contributing to neurodegeneration and exacerbation of neurodegenerative diseases. Noteworthy, previous studies have already suggested exogenous

administration of complex gangliosides GM1 and GD1, *in vitro*, as being beneficial in the recuperation of certain neurodegenerative diseases [45, 46]. The use of enzymes from glycosphingolipid biosynthesis has also been proposed as a therapeutic target for attenuating some symptoms in AD [39].

Furthermore, it is important to clarify the role of oxidative stress on variation of the ganglioside compositions in the neurodegenerative diseases associated to oxidative stress, as Alzheimer's disease. Research in this particular area may lead to the identification of new therapeutic targets or, at least, lead to the development of additional procedures in order to maximize the quality of life of patients.

Conclusions

Nonenzymatic oxidation of GM1 can be associated with the formation of other glycosphingolipids and ceramides. The observed oxidative depolymerization of ganglioside GM1, with formation of GM2, GM3, asialo-GM1, asialo-GM2, LacCer, GlcCer, and Cer, may lead to alterations of concentration of the gangliosides *in vivo* under oxidative stress, causing an imbalance in cellular sphingolipidome and, consequently, abnormalities in cell signaling.

Oxidized products formed by addition of one oxygen atom, as keto and hydroxy derivatives were also observed in this study, as well as glycans, oxidized glycans, and oxidative cleavage between C2 and C3, and between C3 and C4 of the sphingosine backbone. Still, there is a lack the knowledge on the possible formation and on the biological effects of these ganglioside oxidation products in living organisms under oxidative stress. Nevertheless, these findings contribute to a better understanding of the fate of GM1 under oxidative stress and to consider the possibility that GM1 oxidation is contributing to neurodegeneration and inflammation observed in neurodegenerative diseases.

Acknowledgments

Thanks are due to University of Aveiro, Fundação para a Ciência e Tecnologia (FCT, Portugal)/MEC, European Union, QREN, and COMPETE, for funding the QOPNA research unit (project PEst-C/UI0062/2013), and CESAM (UID/AMB/50017/2013), through national funds and where applicable co-financed by the FEDER, within the PT2020 Partnership Agreement, and also to the Portuguese National Mass Spectrometry Network (REDE/1504/REM/2005). T.M. (SFRH/BD/84691/2012), E.M. (SFRH/BPD/104165/2014), and E.A. (BPD/UI51/5441/2015 from RNEM/2013/UA and SFRH/BPD/109323/2015) are grateful to FCT for their grants.

References

1. Kolter, T., Proia, R.L., Sandhoff, K.: Combinatorial ganglioside biosynthesis. *J. Biol. Chem.* **277**, 25859–25862 (2002)
2. Meisen, I., Mormann, M., Müthing, J.: Thin-layer chromatography, overlay technique and mass spectrometry: a versatile triad advancing

- glycosphingolipidomics. *Biochim. Biophys. Acta Mol. Cell Biol. Lipids* **1811**, 875–896 (2011)
3. Lingwood, C.A.: Glycosphingolipid functions. *Cold Spring Harb Perspect. Biol.* **3**, 1–26 (2011)
 4. Ladisch, S., Becker, H., Ulsh, L.: Immunosuppression by human gangliosides. I. Relationship of carbohydrate structure to the inhibition of T cell responses. *Biochim. Biophys. Acta Lipids Lipid Metab.* **1125**, 180–188 (1992)
 5. Cohen, N.R., Garg, S., Brenner, M.B.: Chapter 1. Antigen presentation by CD1. *Adv. Immunol.* **102**, 1–94 (2009)
 6. Brossay, L., Chioda, M., Burdin, N., Koezuka, Y., Casorati, G., Dellabona, P., Kronenberg, M.: CD1d-mediated recognition of an alpha-galactosylceramide by natural killer T cells is highly conserved through mammalian evolution. *J. Exp. Med.* **188**, 1521–1528 (1998)
 7. Sandhoff, K., Kolter, T.: Biosynthesis and degradation of mammalian glycosphingolipids. *Philos. Trans. R. Soc. Lond B Biol. Sci.* **358**, 847–861 (2003)
 8. Nekrasov, E., Hubl, U.: In: *Sialobiology Struct. Biosynth. Funct. Sialic Acid Glycoconjugates Heal. Dis.* (Ed. Martinez-Duncker, J.T. and I.) pp. 313–380 (2013)
 9. Tettamanti, G.: Ganglioside/glycosphingolipid turnover: new concepts. *Glycoconj. J.* **20**, 301–317 (2004)
 10. Thomas, P.D., Brewer, G.J.: Gangliosides and synaptic transmission. *Biochim. Biophys. Acta Rev. Biomembr.* **1031**, 277–289 (1990)
 11. Svennerholm, L.: Gangliosides and synaptic transmission. *Adv. Exp. Med. Biol.* **125**, 533–544 (1980)
 12. Xu, Y.-H., Barnes, S., Sun, Y., Grabowski, G.A.: Multi-system disorders of glycosphingolipid and ganglioside metabolism. *J. Lipid Res.* **51**, 1643–1675 (2010)
 13. Kracun, I., Kalanj, S., Talan-Hranilovic, J., Cosovic, C.: Cortical distribution of gangliosides in Alzheimer's disease. *Neurochem. Int.* **20**, 433–438 (1992)
 14. Rapport, M.M., Donnenfeld, H., Brunner, W., Hungund, B., Bartfeld, H.: Ganglioside patterns in amyotrophic lateral sclerosis brain regions. *Ann. Neurol.* **18**, 60–67 (1985)
 15. Ribas, G.S., Pires, R., Coelho, J.C., Rodrigues, D., Mescka, C.P., Vanzin, C.S., Biancini, G.B., Negretto, G., Wayhs, C.A.Y., Wajner, M., Vargas, C.R.: Oxidative stress in Niemann-Pick type C patients: a protective role of *N*-butyl-deoxyjirimycin therapy. *Int. J. Dev. Neurosci.* **30**, 439–444 (2012)
 16. Haughey, N.J., Bandaru, V.V.R., Bae, M., Mattson, M.P.: Roles for dysfunctional sphingolipid metabolism in Alzheimer's disease neuropathogenesis. *Biochim. Biophys. Acta* **1801**, 878–886 (2010)
 17. Gandhi, S., Abramov, A.Y.: Mechanism of oxidative stress in neurodegeneration. *Oxidative Med. Cell. Longev.* **2012**, 428010 (2012)
 18. Domingues, M.R.M., Reis, A., Domingues, P.: Mass spectrometry analysis of oxidized phospholipids. *Chem. Phys. Lipids* **156**, 1–12 (2008)
 19. Catalá, A.: Lipid peroxidation of membrane phospholipids generates hydroxy-alkenals and oxidized phospholipids active in physiological and/or pathological conditions. *Chem. Phys. Lipids* **157**, 1–11 (2009)
 20. Kinnunen, P., Hermetter, A., Spickett, C.M., Reis, A., Spickett, C.M.: Chemistry of phospholipid oxidation. *Biochim. Biophys. Acta Biomembr.* **1818**, 2374–2387 (2012)
 21. Maciel, E., Domingues, P., Domingues, M.R.M.: Liquid chromatography/tandem mass spectrometry analysis of long-chain oxidation products of cardiolipin induced by the hydroxyl radical. *Rapid Commun. Mass Spectrom.* **25**, 316–326 (2011)
 22. Melo, T., Maciel, E., Oliveira, M.M., Domingues, P., Domingues, M.R.M.: Study of sphingolipids oxidation by ESI tandem MS. *Eur. J. Lipid Sci. Technol.* **114**, 726–732 (2012)
 23. Yurkova, I., Kisel, M., Arnhold, J., Shadyro, O.: Free-radical fragmentation of galactocerebrosides: a MALDI-TOF mass spectrometry study. *Chem. Phys. Lipids* **134**, 41–49 (2005)
 24. Couto, D., Santinha, D., Melo, T., Ferreira-Fernandes, E., Videira, R.A., Campos, A., Fardilha, M., Domingues, P., Domingues, M.R.M.: Glycosphingolipids and oxidative stress: evaluation of hydroxyl radical oxidation of galactosyl and lactosylceramides using mass spectrometry. *Chem. Phys. Lipids* **191**, 106–114 (2015)
 25. Vázquez, M.C., Balboa, E., Alvarez, A.R., Zanlungo, S.: Oxidative stress: a pathogenic mechanism for Niemann-Pick type C disease. *Oxidative. Med. Cell. Longev.* **2012**, 1–11 (2012)
 26. Castro, B.M., Prieto, M., Silva, L.C.: Ceramide: a simple sphingolipid with unique biophysical properties. *Prog. Lipid Res.* **54**, 53–67 (2014)
 27. Wu, B.X., Clarke, C.J., Hannun, Y.A.: Mammalian neutral sphingomyelinases: regulation and roles in cell signaling responses. *Neuromol. Med.* **12**, 320–330 (2010)
 28. Ito, E., Tominaga, A., Waki, H., Miseki, K., Tomioka, A., Nakajima, K., Kakehi, K., Suzuki, M., Taniguchi, N., Suzuki, A.: Structural characterization of monosialo-, disialo-, and trisialo-gangliosides by negative ion AP-MALDI-QIT-TOF mass spectrometry with MS(n) switching. *Neurochem. Res.* **37**, 1315–1324 (2012)
 29. Merrill, A.H., Sullards, M.C., Allegood, J.C., Kelly, S., Wang, E.: Sphingolipidomics: high-throughput, structure-specific, and quantitative analysis of sphingolipids by liquid chromatography tandem mass spectrometry. *Methods* **36**, 207–224 (2005)
 30. Ii, T., Ohashi, Y., Nagai, Y.: Structural elucidation of underivatized gangliosides by electrospray-ionization tandem mass spectrometry (ESIMS/MS). *Carbohydr. Res.* **273**, 27–40 (1995)
 31. Tudella, J., Nunes, F.M., Paradelo, R., Evtuguin, D.V., Domingues, P., Amado, F., Coimbra, M.A., Barros, A.I.R.N.A., Domingues, M.R.M.: Oxidation of mannosyl oligosaccharides by hydroxyl radicals as assessed by electrospray mass spectrometry. *Carbohydr. Res.* **346**, 2603–2611 (2011)
 32. Santinha, D., Ferreira-Fernandes, E., Melo, T., Silva, E.M.P., Maciel, E., Fardilha, M., Domingues, P., Domingues, M.R.M.: Evaluation of the photo-oxidation of galactosyl- and lactosylceramide by electrospray ionization mass spectrometry. *Rapid Commun. Mass Spectrom.* **28**, 2275–2284 (2014)
 33. Ann, Q., Adams, J.: Structure-specific collision-induced fragmentations of ceramides cationized with alkali-metal ions. *Anal. Chem.* **65**, 7–13 (1993)
 34. Domon, B., Costello, C.E.: Structure elucidation of glycosphingolipids and gangliosides using high-performance tandem mass spectrometry. *Biochemistry* **27**, 1534–1543 (1988)
 35. Ann, Q., Adams, J.: Structure determination of ceramides and neutral glycosphingolipids by collisional activation of $[M + Li]^+$ ions. *J. Am. Soc. Mass Spectrom.* **3**, 260–263 (1992)
 36. Yurkova, I.L.: Free-radical reactions of glycerolipids and sphingolipids. *Russ. Chem. Rev.* **81**, 175–190 (2012)
 37. Ando, S., Chang, N.-C., Yu, R.K.: High-performance thin-layer chromatography and densitometric determination of brain ganglioside compositions of several species. *Anal. Biochem.* **89**, 437–450 (1978)
 38. Palmano, K., Rowan, A., Guillermo, R., Guan, J., McJarrow, P.: The role of gangliosides in neurodevelopment. *Nutrients* **7**, 3891–3913 (2015)
 39. Yu, R.K., Tsai, Y.-T., Ariga, T.: Functional roles of gangliosides in neurodevelopment: an overview of recent advances. *Neurochem. Res.* **37**, 1230–1244 (2012)
 40. Caughlin, S., Hepburn, J.D., Park, D.H., Jurcic, K., Yeung, K.K.-C., Cechetto, D.F., Whitehead, S.N.: Increased expression of simple ganglioside species GM2 and GM3 detected by MALDI imaging mass spectrometry in a combined rat model of A β toxicity and stroke. *PLoS One* **10**, e0130364 (2015)
 41. Filippov, V., Song, M.A., Zhang, K., Vinters, H.V., Tung, S., Kirsch, W.M., Yang, J., Duerksen-Hughes, P.J.: Increased ceramide in brains with Alzheimer's and other neurodegenerative diseases. *J. Alzheimers Dis.* **29**, 537–547 (2012)
 42. Cutler, R.G., Kelly, J., Storie, K., Pedersen, W.A., Tammara, A., Hatanpaa, K., Troncoso, J.C., Mattson, M.P.: Involvement of oxidative stress-induced abnormalities in ceramide and cholesterol metabolism in brain aging and Alzheimer's disease. *Proc. Natl. Acad. Sci. U. S. A.* **101**, 2070–2075 (2004)
 43. Shadyro, O., Yurkova, I., Kisel, M., Brede, O., Arnhold, J.: Formation of phosphatidic acid, ceramide, and diglyceride on radiolysis of lipids: identification by MALDI-TOF mass spectrometry. *Free Radic. Biol. Med.* **36**, 1612–1624 (2004)
 44. Czubowicz, K., Strosznajder, R.: Ceramide in the molecular mechanisms of neuronal cell death. The role of sphingosine-1-phosphate. *Mol. Neurobiol.* **50**, 26–37 (2014)
 45. Kreutz, F., Frozza, R.L., Breier, A.C., de Oliveira, V.A., Horn, A.P., Pettenuzzo, L.F., Netto, C.A., Salbego, C.G., Trindade, V.M.T.: Amyloid- β induced toxicity involves ganglioside expression and is sensitive to GM1 neuroprotective action. *Neurochem. Int.* **59**, 648–655 (2011)
 46. Schneider, J.S., Gollomp, S.M., Sendek, S., Colcher, A., Cambi, F., Du, W.: A randomized, controlled, delayed start trial of GM1 ganglioside in treated Parkinson's disease patients. *J. Neurol. Sci.* **324**, 140–148 (2013)